



HAL
open science

A STUDY OF THE INFLUENCE OF THE WIDTH OF CUT ON MICRO MILLING ALUMINUM ALLOY

Anna Carla Araujo, Adriane Lopes Mougo, Fabio Oliveira Campos

► To cite this version:

Anna Carla Araujo, Adriane Lopes Mougo, Fabio Oliveira Campos. A STUDY OF THE INFLUENCE OF THE WIDTH OF CUT ON MICRO MILLING ALUMINUM ALLOY. 22nd International Congress of Mechanical Engineering (COBEM 2013), Nov 2013, Ribeirão Preto, Brazil. hal-03214837

HAL Id: hal-03214837

<https://hal.science/hal-03214837>

Submitted on 3 May 2021

HAL is a multi-disciplinary open access archive for the deposit and dissemination of scientific research documents, whether they are published or not. The documents may come from teaching and research institutions in France or abroad, or from public or private research centers.

L'archive ouverte pluridisciplinaire **HAL**, est destinée au dépôt et à la diffusion de documents scientifiques de niveau recherche, publiés ou non, émanant des établissements d'enseignement et de recherche français ou étrangers, des laboratoires publics ou privés.



A STUDY OF THE INFLUENCE OF THE WIDTH OF CUT ON MICRO MILLING ALUMINUM ALLOY

Adriane Lopes Mougo

Fábio de Oliveira Campos

Anna Carla Monteiro de Araujo

CEFCON Machining Research Laboratory

Mechanical Engineering Department, COPPE/UFRJ, Rio de Janeiro, Brazil

adriane.mougo@gmail.com

fabiocampos23@bol.com.br

anna@mecanica.ufrj.br

Abstract. *The minimum chip thickness is the lower limit value where cutting process occurs as it is studied in cutting metal. Below this value the process is usually modeled as forming. In micro end milling the chip thickness varies with the rotation angle from zero to the feed per tooth. This article presents a first effort to divide the cutting process in two phases: when the chip thickness is below the lower limit and when there is cutting mechanism. It is proposed to calculate differently those two forces: forming forces and cutting forces. It is presented an experimental study on micro milling aluminum alloy with different width of cut in order to identify the influence of the minimum chip thickness on the resultant forces. Using lower width of cut, the time during forming phase would be relatively higher. Experimental data is acquired using a micro dynamometer and the forces are analyzed. Tool wear and workpiece surface features were also investigated. The design of experiments considers one factor, the width of cut, with four levels. The machined workpiece showed good superficial quality for lower width of cut with less burr formation along the channel.*

Keywords: *Micro milling, width of cut, cutting forces, tool wear, workpiece surface features.*

1. INTRODUCTION

Micro milling is a flexible machining process that allows the fabrication of high quality parts. Cutting force analysis plays a vital role in studying the micro milling processes. Micro milling is a suitable process for producing complex 3D geometries for a wide range of materials, so the understanding the physical phenomena affecting the process performance is essential in order to increase the quality of the micro-milled components (Afazov *et al.*, 2013).

The size of the part in machining of metallic components plays an important role in the force prediction. The fundamental process mechanisms between macro and microcutting can be different due to the substantial size reduction. This is known as the “size effect” in micro machining (Aramcharoen and Mativenga, 2009). The feed per tooth to tool radius ratio has to be higher than in conventional milling to keep productivity at a reasonable level (Bao and Tansel, 2000). Due to the small size of the micro-tools, which have a diameter of less than 2 mm, it is very difficult to notice the damage in the cutting edges and an inappropriate selection of the cutting conditions can cause tool breakage unexpectedly.

Even if the relationship between the main geometrical features is kept constant, the process behavior changes. Vollertsen *et al.* (2009) presented a review on size effect and their use: the article presents the typology of size effects, a description of size effects on strength and tribology and size effects on formability and machinability. Camara *et al.* (2012) presented a state of art on micro milling with emphasis on the work material requirements, tool materials and geometry, cutting forces and temperature, quality of the finished product, burr formation, process modeling and monitoring and machine tool requirements. Afazov *et al.* (2013) studied the micro milling conditions on the cutting forces and process stability through the effects of the tool wear, rake angle, run-out and workpiece material.

At low feed rates, when chip thickness (t_c) is lower than the required minimum chip thickness (t_{cmin}), rubbing or ploughing occurs instead of cutting (Bayesteh *et al.*, 2013). A critical cutting thickness needs to be exceeded to promote the chip removal. Ramos *et al.* (2012) studied the transition from ploughing to cutting in micromachining and evaluated the minimum uncut chip thickness. In this study the changes of the surface roughness, surface topography and residual stress state after micro cutting have been also investigated. If the chip thickness is below this value ($t_c < t_{cmin}$), the ploughing mechanism is present, where part of the material is plastically pushed against the workpiece surface. It is also possible to have the elasticity mechanism when the forces are lower. In this case, $t_c \ll t_{cmin}$ and the forces are proportional to the interference volume between the tool and the workpiece (Vogler *et al.*, 2004). Similarly, Malekian *et al.* (2012) used the minimum uncut chip thickness, under which the material is not removed but ploughed, and claimed that this effect causes an increase of machining forces that affect the surface integrity of the workpiece.

Microstructure has also a significant effect on microscale cutting. Simoneau *et al.* (2007) investigates the effect of grain size and orientation during microcutting in FE modeling of the primary shear zone. Their research group (Simoneau *et al.*, 2006) analyzed the orthogonal cutting in microscale. Tests were conducted on steel and the resulting

A. L. Mougo, A. C. Araujo, F. O. Campos
Effect of Width of cut on Micro Milling Aluminum Alloy

chips examined showing that the chip formation changes from continuous to “quasi-shear-extrusion” chip due to the uncut thickness size. The results indicate that the pearlite and softer ferrite grains play distinct roles in the plastic deformation process. Araujo *et al.* (2013) studied the micro milling cutting forces on machining aluminum alloy and experimental results were compared to mechanistic model.

Literature review shows the assumption of non-homogeneity in workpiece material properties because the micro-grain-structure size is of the same order of magnitude as the cutter radius of curvature and the grain structures will affect the cutting properties (Afazov *et al.*, 2013, Camara *et al.*, 2012, Simoneau *et al.*, 2007). However, the study of the size effect considering the homogeneous material properties is important to reduce the experimental and simulated conditions in micromachining.

This article presents an experimental study on micro milling aluminum alloy using different width of cut. Cutting Forces, burr formation and tool breakage is analyzed and presented. It is proposed to analyze forces reducing the width of cut with the aim to focus on influence of the ploughing phase in the total cutting force.

2. CUTTING FORCE IN MICRO MILLING

The knowledge of cutting forces is fundamental for tool optimization and it is very important to avoid tool breakage and instability. In micro milling, those factors are even more relevant due to the high cost of tools that breaks very easily. Meso and micro milling models are presented.

2.1 General chip load cutting model for cutting forces

Elemental normal and frictional forces are required to the determination of cutting forces for a given geometry. The mechanistic modeling approach is a combination of analytical and empirical methods in which the forces are proportional to the chip load (Kline *et al.*, 1982).

The specific cutting pressure, K_n , K_f and K_z (tangential, radial and axial coefficients respectively), have been shown as a function of chip thickness t_c in mesoscale milling process and it is used for calculation of the differential cutting forces dF_n , dF_f and dF_z on each angular position θ of the discretized cutting edge proportional to the chip load area dA as shown in Eq. 1.

$$\begin{aligned}dF_t(\theta) &= k_t dA(\theta) \\dF_r(\theta) &= m_1 k_t dA(\theta) \\dF_z(\theta) &= m_2 k_t dA(\theta)\end{aligned}\tag{1}$$

Using a semi empirical modeling as Tlustý and MacNeil (1975), relating specific cutting pressures by empiric factors m_1 and m_2 . Chip area is calculated based on uncut chip thickness $t_c(\theta)$ that is called Martellotti equation.

$$t_c(\theta) = f_t \sin(\theta)\tag{2}$$

where f_t is the feed per tooth.

The specific cutting pressure in mechanistic models is calculated as:

$$\ln k_t = a_0 + a_1 \ln t_c + a_2 \ln V_c + a_3 \ln t_c \ln V_c\tag{3}$$

where the coefficients a_0 , a_1 , a_2 and a_3 are called specific cutting energy coefficients and they need to be experimentally calculated. They are dependent on the tool and workpiece materials and also on the cutting speed and the chip thickness. Those coefficients are determined from calibration tests for a given tool work piece combination and for a given range of cutting conditions.

2.2 Cutting force model using chip load and cutting edge

Other models consider that the cutting edge length influence the cutting force. The differential tangential, radial and axial cutting forces can be composed by one parcel that it is dependent of the cutting area and another that is proportional to the cutting edge db , as in Eq. 4 (Pérez *et al.*, 2007).

$$\begin{aligned}
 dF_t(\theta) &= k_{tc} t_c(\theta) db + k_{te} db \\
 dF_r(\theta) &= m_1 k_{rc} t_c(\theta) db + k_{re} db \\
 dF_z(\theta) &= m_2 k_{zc} t_c(\theta) db + k_{ze} db
 \end{aligned} \tag{4}$$

where k_{tc} , k_{rc} and k_{zc} are the cutting forces coefficients in the tangential, radial and axial directions, and k_{te} , k_{re} and k_{ze} are the edge forces coefficients in the same directions.

2.3 Cutting force model considering chip thickness correction for microcutting

Bao and Tansel (2000) developed a more precise expression than Martelotti calculation for uncut chip thickness $t_c(\theta)$ used by Newby *et al.* (2007) to calculate average uncut thickness, as shown in Eq. 5. This equation can be used to replace $t_c(\theta)$ in the Eq. (1) or (4).

$$t_c(\theta) = f_i \sin(\theta) - \frac{z}{2nr} f_i^2 \sin(\theta) \cos(\theta) + \frac{f_i^2}{2f} \cos^2(\theta) \tag{5}$$

where z , n and r are the tool teeth, spindle speed and tool radius respectively.

2.4 Minimum uncut chip thickness for cutting force prediction

Under the minimum uncut chip thickness, ploughing mechanism is present and it needs to be modeled by different approaches than the presented cutting ones. Liu *et al.* (2006) modeled the minimum chip thickness, cutting temperature, strain, and strain rate simultaneously, considering analytical model using slip line theory and Johnson-Cook model. Malekian *et al.* (2012) presented an analytical models based on identifying the stagnant point of the workpiece material during the machining, based on the edge radius r_e and on a critical or stagnant angle, θ_m to calculate t_{cm} .

$$t_{cm} = r_e (1 - \cos \theta_m) \tag{6}$$

The stagnant angle is considered by Malekian *et al.* (2012) to be equal to the friction angle between the material and the rake face, regardless of the other parameters involved in the process and the edge radius can be either measured or by the tool manufacturer.

A trigonometric analysis is used to calculate the minimal width of cut ($a_{e\min}$), using Eq. (2) and (7), that defines when the material begins to be removed. This calculation considers the tool radius (R) and the tool rotation angle θ_m for this minimum width of cut. Figure 1 represents the relation between the width of cut a_e and the tool rotation angle θ_m for any case.

$$a_e = R(1 - \cos \theta_m) \tag{7}$$

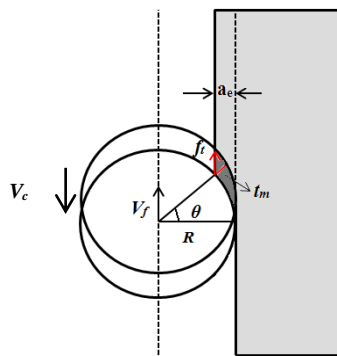


Figure 1. Relation between the width of cut a_e and the tool rotation angle θ .

The rotation angle assumes values from zero to 2π if there is full immersion, when $a_e=2R=D$. In this case, for $\theta < \theta_m$ and $\theta > 2\pi - \theta_m$ the milling process contains only ploughing mechanism. When $\theta_m < \theta < 2\pi - \theta_m$, cutting process is running. For values of the width of cut smaller than D , the cutting force analysis must be aware on the impact of this

ploughing phase on process, as shown in Fig. 2. This article deals with experimental procedure with different values of a_c in order to study the tool and process behavior on each case.



Figure 2. Shearing and ploughing areas when $a_c=2R=D$ (Bayesteh *et al.*, 2013).

3. EXPERIMENTAL SETUP

In order to analyze the cutting forces involved in the process of micro milling with different width of cut, a series of experiments were performed.

3.1 Material, tools and experiments

The work material used on experiments is the alloy Al 6351 T6, which is an AlMgSi alloy. The workpiece dimensions were 47x50x15 mm. It was used a carbide micro milling tool, with 0.254 mm diameter and 0.762 mm flute length, as showed in Fig. 3.

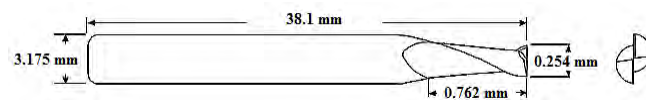


Figure 3. Dimensions of the micro milling tool used on the experiments.

The cutting tool was measured in SEM microscopy. As the cutting edge radius has strong influence on the cutting force, the images presented on Fig. 4 were taken. Using those SEM images, the helix angle, point radius and cutting edge radius are measured. The tool has point tip radius of 1.58 μm , cutting edge radius of 0.53 μm and $\beta=30^\circ$ helix angle.

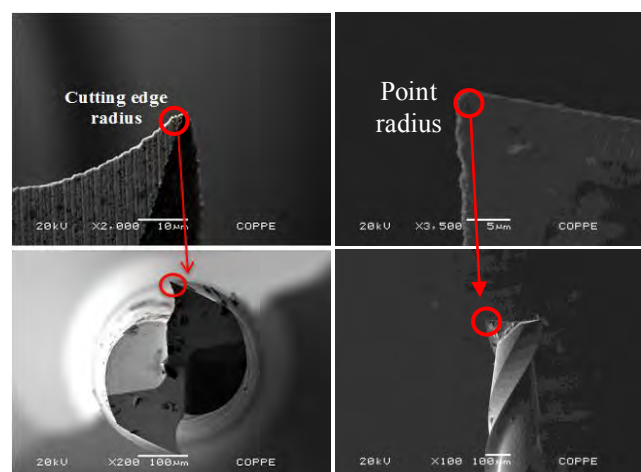


Figure 4: SEM Microscopy of the cutting tool presenting the cutting edge radius and the point radius.

CNC Mini Mill/GX from Minitech Machinery Corporation was used on the experiments. The machine uses NSK 60K RPM Precision Spindle with 3 Axis Controller. Its standard resolution is 0.78125 μm using dual linear ball bearing slides on each axis, sealed for the table mechanism (THK linear slides - RSR15 series, Caged-ball technology). The drive mechanism THK Ball Screw actuator - preloaded and sealed, achieves low torque fluctuation and no backlash.

A mini-dynamometer is used for cutting force measurement. The MiniDyn KISTLER 9256C2 used cable 1697A5 and the cutting forces components are presented in Fig. 5a. It was used a charge amplifier 5070A10100 and a data

acquisition board NI USB 6251. The mini-dynamometer was calibrated with a sensitivity of -25.61 pC/N on F_x , -12.86 pC/N on F_y and -25.86 pC/N on F_z . The frequency of data acquisition was 40000 Hz and an amplifying rate of 2 N/V was used on the charge amplifier. An optical profilometer for surface flatness and roughness measurement of Taylor Hobson, model CCI MP, is used for topography measurement.

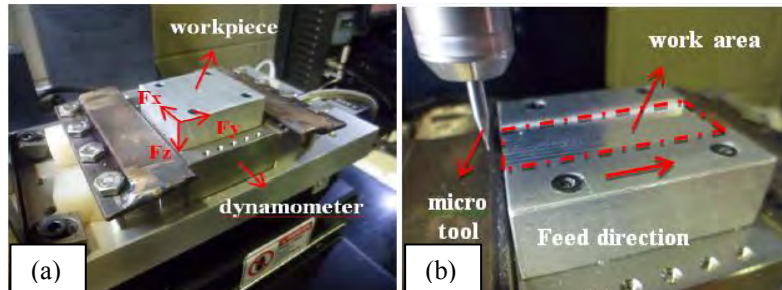


Figure 5. Experimental set-up: (a) Mini Dyn and force components; (b) Feed directions.

3.2 Experimental procedure

Before the actual micro milling experiments started, a surface of $50 \times 20 \text{ mm}$, the work area, was faced on the workpiece using a 3 mm milling tool, as shown in the Fig. 5b. It was used 18 m/min as cutting velocity and feed rate equals to 200 mm/min . This facing operation is important because it ensures that the micro milling operation would be performed on a flat surface. If the surface to be machined was not flat, the axial depth of cut could vary during the cutting process and, consequently, the forces data would not be right.

The micro milling tool performed a surface trajectory before each pass to guarantee the axial depth of cut designed. The axial depth of cut chosen is 30 times higher than the point radius, $50 \text{ }\mu\text{m}$. The feed per tooth chosen is 4 times higher than the cutting edge radius, $2 \text{ }\mu\text{m}$, to ensure the removal of material. Table 1 presents the cutting parameters used on the experiments.

Table 1: Cutting parameters.

Cutting Velocity (V_c)	23.93 m/min - clockwise
Feed per tooth (f_z)	$2 \text{ }\mu\text{m/tooth}$
Axial depth of cut (a_p)	$50 \text{ }\mu\text{m}$
Width of cut (a_c)	$254 \text{ }\mu\text{m}$ (full immersion)
Workpiece material	Al 6351 T6

Initially, four channels were machined with a micro-end-milling process, using full immersion and spaced by 1.5 mm in between, as shown in Fig. 6. For the design of experiment the values of a_c were selected considering the cut tool diameter (D). The width of cut used to machine channels 1 to 4 were $12,5\% D$, $25\% D$, $50\% D$ and $100\% D$, as presented in Tab. 2.

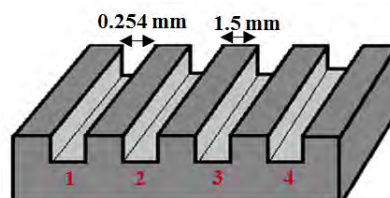


Figure 6: Scheme for channels machined for testing.

Table 2: Design of Experiments.

Channel	Relation with D	Value of a_c (mm)	Value of θ (rad)
1	$12,5\%$	0.0318	0.72
2	25%	0.0635	1.05
3	50%	0.1270	1.57
4	100%	0.2540	3.14

The channel 4 remains with $a_c = D$ for the comparison with the others channels, as shown in Fig. 7. With Eq. (2) it is possible to calculate the value of $\theta_{\min}=0.268$ rad, considering $t_c(\theta)=0.53$ μm and $f_t=2\mu\text{m/tooth}$. With Eq. (6) and (7) it is possible to calculate the values of $t_{\text{cm}}=0.02$ μm and $a_{\text{emin}}=4.57$ μm , considering $r_e=0.53$ μm and $R=127$ μm .

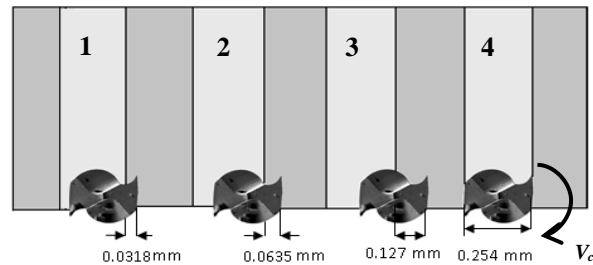


Figure 7: Machining of channels with different a_c .

4. RESULTS AND DISCUSSION

In this section, experimental cutting force, tool wear and micro-machined surfaces characteristics will be presented.

4.1 Cutting forces

The experimental cutting forces were obtained with a media of 20 rotations on each experiment. The signal was filtered using a high-pass filter with the cut-off frequency corresponding to the frequency of the spindle speed. Figure 8 show the force signals in the X and Y directions. The force components presented (F_x and F_y) represents the components on the plane normal to the spindle, as presented on Fig 5a. The profile of the cutting forces presented influence of noise for all channels, especially for values of cutting force with $a_c < D$.

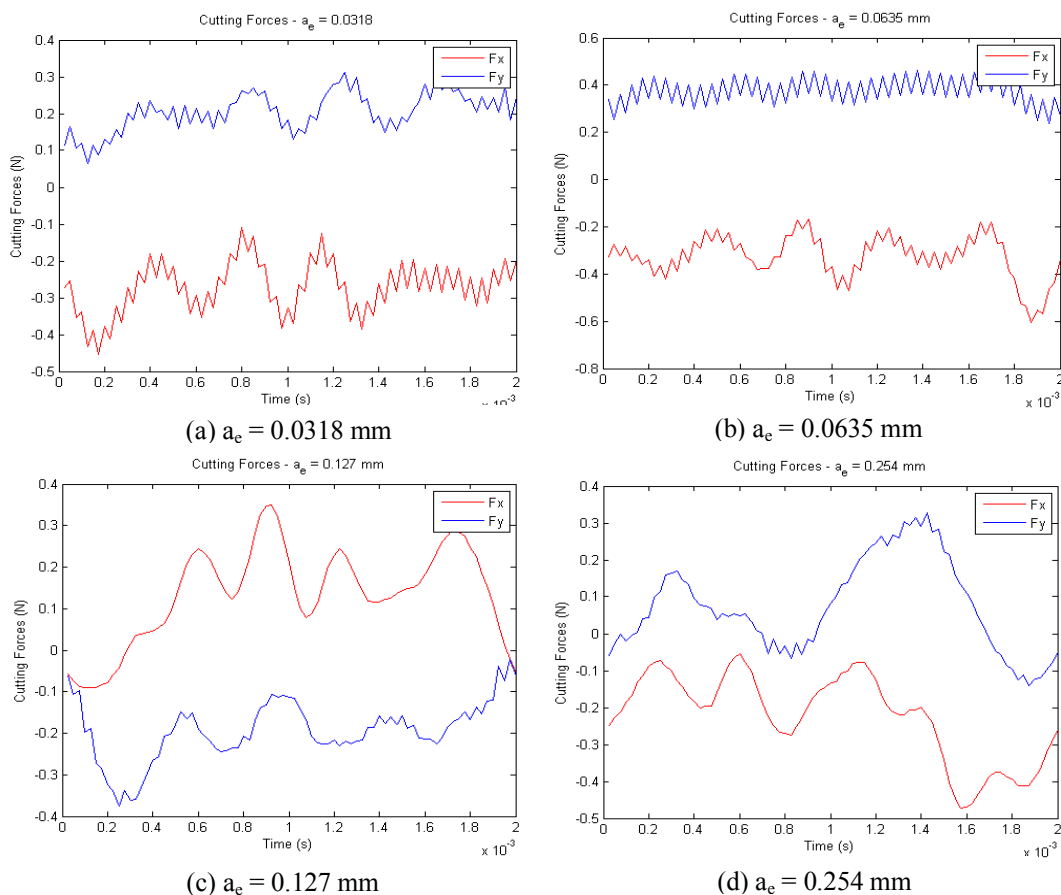


Figure 8. Experimental cutting forces.

Figure 8 shows that for very low values of a_e or even with full immersion, the relation signal/noise is low, influenced either by the feed rate or by the spindle speed, or by both.

4.2 Tool wear

The wear and the modification in the geometry of the cutting edge increase the vibration during material removal, inducing the formation of burr. After the experiments, it was verified that the cutting point of the tool was broken, as showed in Fig. 9a. Figure 9b presents the EDS (Energy Dispersive Spectroscopy) at pt2, indicating the presence of aluminum chips on the cutting face.

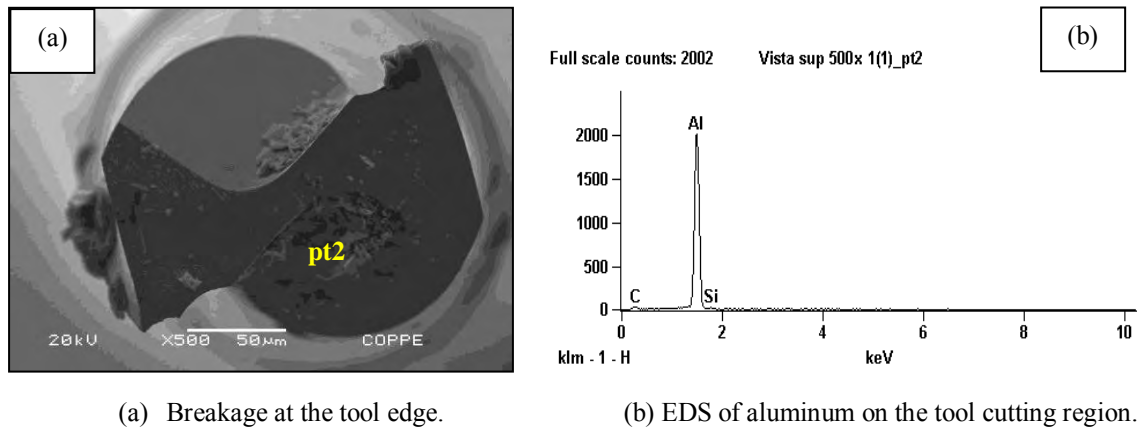
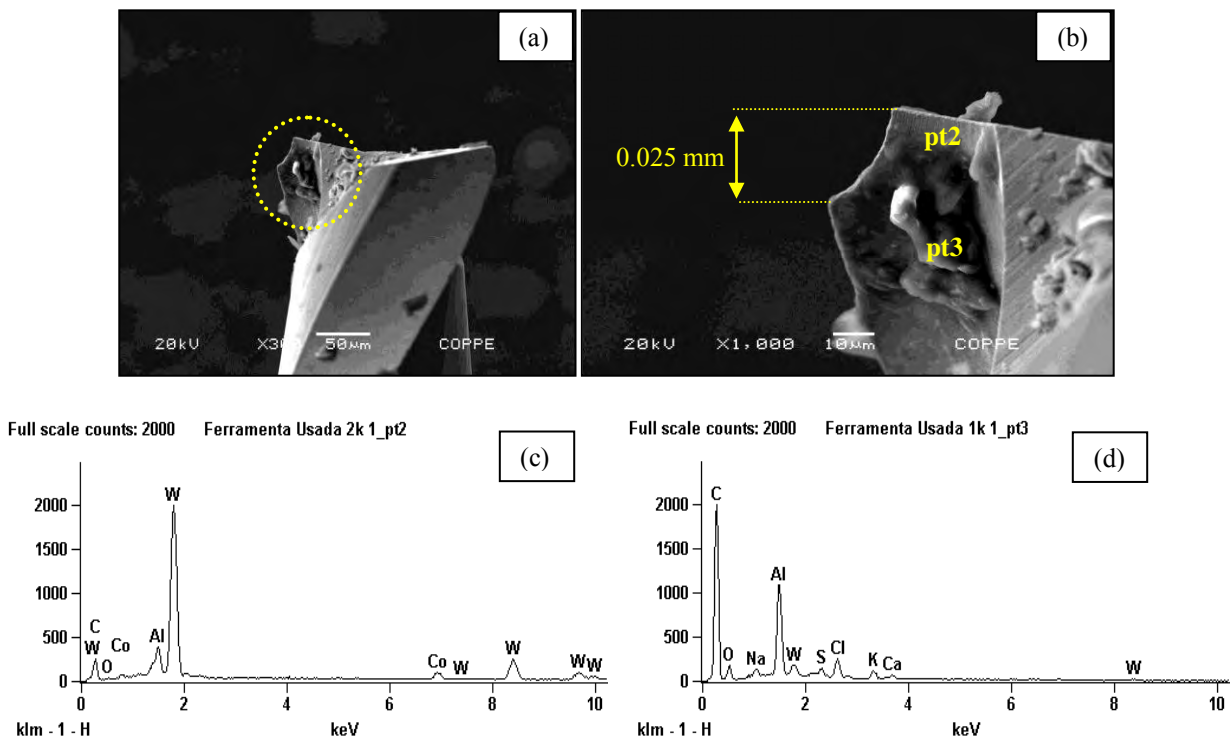


Figure 9. Tool analysis on top view.

Figures 10a and 10b present the break of the tool point in 0.0025 mm, in front view. Figures 10c and 10d show EDS at point pt2 and pt3, indicating the tungsten and the presence of aluminum on the tool.



4.3 Workpiece surface features

Figure 11 shows the 4 channels machined with width of cut variation. Channels 1, 2 and 3 present good surface finishing and channel 4, machined at full immersion of the tool ($a_e = D = 0.254$ mm), showed high burr occurrence.

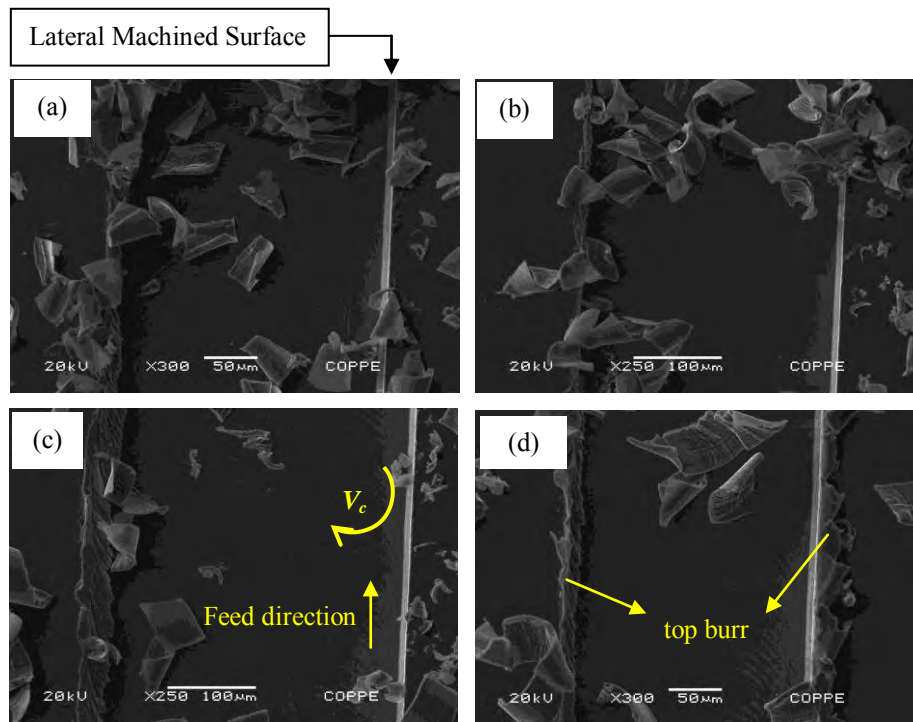


Figure 11. Front view of the channels. (a) Channel 1 with $a_e = 0.0318$ mm, (b) Channel 2 with $a_e = 0.0635$ mm, (c) Channel 3 with $a_e = 0.127$ mm e (d) Channel 4 with $a_e = 0.254$ mm.

Figure 12 presents the top view of channels 2 and 4 at the start and at the end of cutting. There was burr formation only at channel 4. The breakage of the tool point, the adhesion of aluminum on the cutting face and the selection of the cutting parameters can cause these burrs.

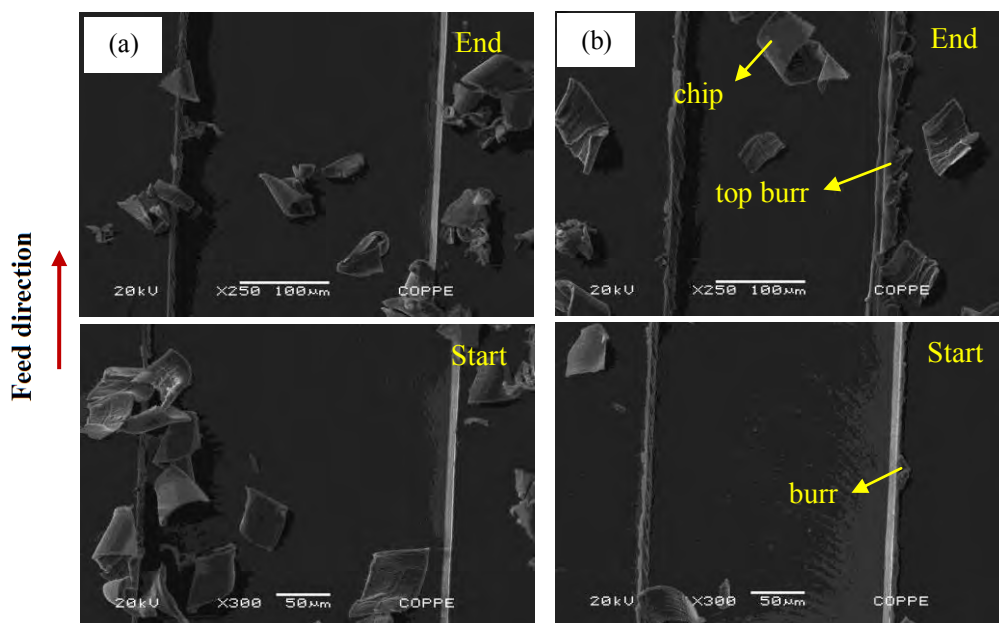


Figure 12. Start and end of channel cutting. (a) Channel 2 with $a_e = 0.0635$ mm e (b) Channel with 4 $a_e = 0.254$ mm.

Figure 13 presents the side view of channels 2 and 4 at the starting of the cutting of the channel. Channel 4 shows $a_e = 0.230$ mm, though the tool diameter is 0.254 mm, and this value can be influenced by the presence of burrs. Channel 2 shows $a_e = 0.292$ mm, because of this the difference between the two width of cut is 0.0621 mm. This result shows that the breakage of tool point did not harmed the surface machining of the workpiece.

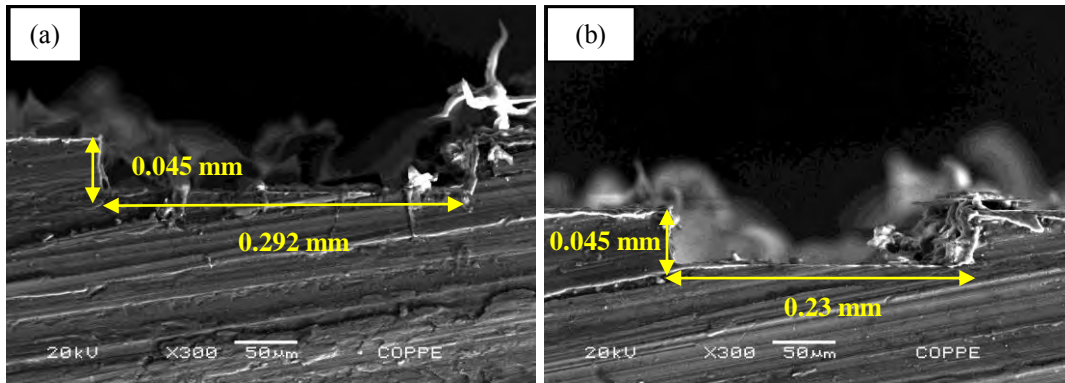
(a) Canal 2 com $a_e = 0.0635$ mm(b) Canal 4 com $a_e = 0.254$ mmFigure 13. Side view of the workpiece. (a) $a_e = 0.0635$ mm and (b) $a_e = 0.254$ mm

Figure 14 shows the topography measurements on each channel. Channel 1, 2, 3 and 4 presents the arithmetic average height (S_a) of 0.252 μm , 0.172 μm , 0.156 μm and 0.170 μm respectively. This results show that the width of cut has stronger effect on the surface quality, and that lower width of cut increases the values of S_a .

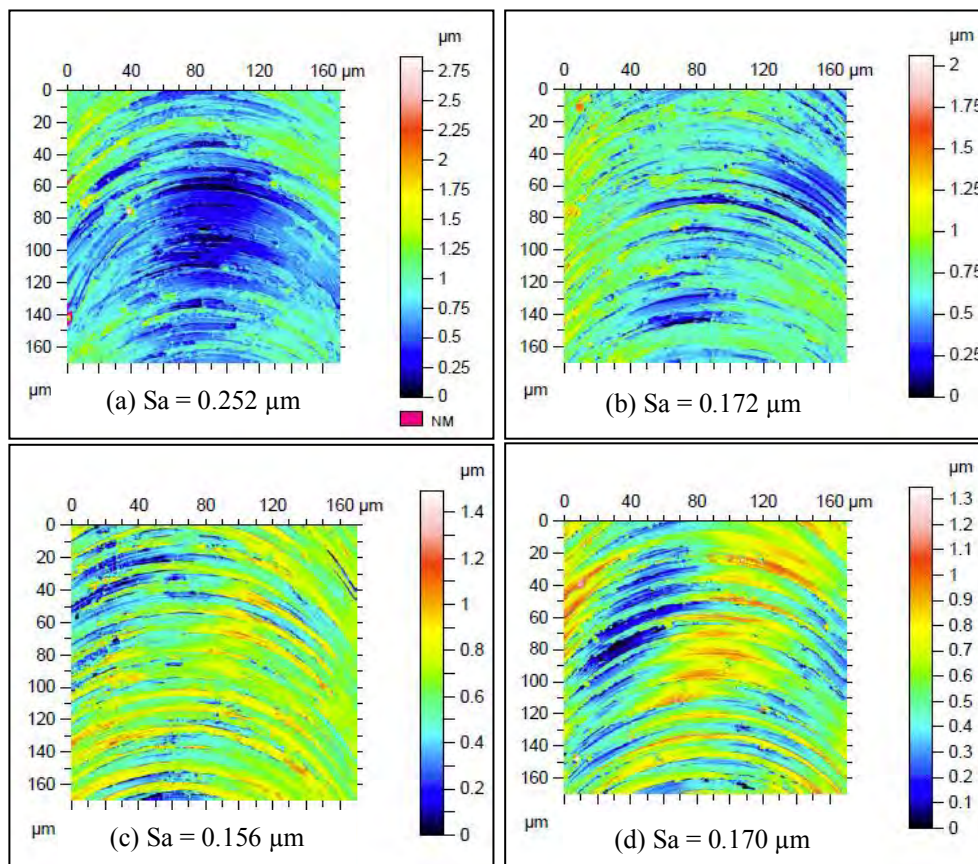


Figure 14. Topography measurement.

5. CONCLUSIONS

In this article it was presented the cutting forces, the tool conditions and the workpiece surface features for micro milling of an aluminum alloy, varying the width of cut. The minimum width of cut calculated was $4.57\ \mu\text{m}$ and in the work were used values between $254\ \mu\text{m}$ and $32\ \mu\text{m}$. However, even with high values, the profile of the cutting forces presented influence of noise, indicating the necessity of an increase at the amplifying rate of the signals.

It was verified the breakage of the tool point, that can be consequence of the selected cutting parameters or of the length of the machined surface, which was $350\ \text{mm}$ for the machining of the channels and the variation of the width of cut.

The machined workpiece showed good superficial quality for width of cut lower than the tool diameter. With width of cut equals to the diameter, there was burr formation along all channels, influenced by the breakage of the tool point. Therefore, with the conditions presented in this work, it is recommended the machined of the channel with a tool with lower diameter and, than, the variation of width of cut for the finishing.

Future works aim the development of a model that considers the different paths of the cutting edge on the workpiece, identifying the moments of ploughing and cutting during the process. For this work, it will be used an equipment with higher amplifying rate, enabling the force acquisition for lower values of feed per tooth and width of cut.

6. ACKNOWLEDGEMENTS

The authors thank to the support of CAPES for acquiring the equipment used in this article thru Pro-equipment resources, to the kindly services of UFRJ importation department for the Mechanical Engineering Department.

7. REFERENCES

- Afazov, S.M., Zdebski, D., Ratchev, S.M., Segal, J., Liu, S., 2013. "Effects of micro milling conditions on the cutting forces and process stability". *Journal of Materials Processing Technology*, Vol. 213, pp. 671-684.
- Aramcharoen, A., Mativenga, P.T., 2009. "Size effect and tool geometry in micromilling of tool steel". *Precision Engineering*, Vol. 33, pp. 402-407.
- Araujo, A.C., Mouro, A.L., Campos, F.O., 2013. "Micro milling forces on machining aluminum alloy". In *8th International Conference on MicroManufacturing – ICOMM2013*. Victoria, Canada
- Bao, W. and Tansel, I., 2000. "Modeling micro-end-milling operations. part i: analytical cutting force model". *International Journal of Machine Tools and Manufacture*, Vol. 40, No. 15, pp. 2155 – 2173.
- Bayesteh, A., Gym, D., Jun, M.B.G., 2013. "2-Dimensional ploughing simulation model development in micro flat end milling". In *8th International Conference on MicroManufacturing – ICOMM2013*. Victoria, Canada.
- Câmara, M., Rubio, J.C., Abrão, A. and Davim, J., 2012. "State of the art on micro milling of materials, a review". *Journal of Materials Science & Technology*, Vol. 28, No. 8, pp. 673 – 685.
- Kline, W., DeVor, R. and Lindberg, J., 1982. "The prediction of cutting forces in end milling with application to cornering cuts". *International Journal of Machine Tool Design and Research*, Vol. 22, No. 1, pp. 7 – 22.
- Liu, X., Devor, R.E. and Kapoor, G., 2006. "An analytical model for the prediction of minimum chip thickness in micromachining". *Trans. ASME*, Vol. 128, pp. 474 – 481.
- Malekian, M., Mostofa, M., Park, S. and Jun, M., 2012. "Modeling of minimum uncut chip thickness in micro machining of aluminum". *Journal of Materials Processing Technology*, Vol. 212, No. 3, pp. 553 – 559.
- Newby, G., Venkatachalam, S., Liang, S.Y., 2007. "Empirical analysis of cutting force constants in micro-end-milling operations". *Journal of Materials Processing Technology*, Vol. 192–193, pp. 41-47.
- Pérez, H., Vizán, A., Hernandez, J. and Guzmán, M., 2007. "Estimation of cutting forces in micromilling through the determination of specific cutting pressures". *Journal of Materials Processing Technology*, Vol. 190, pp. 18-22.
- Ramos, A.C., Autenrieth, H., Strauß, T., Deuchert, M., Hoffmeister, J. and Schulze, V., 2012. "Characterization of the transition from ploughing to cutting in micro machining and evaluation of the minimum thickness of cut". *Journal of Materials Processing Technology*, Vol. 212, No. 3, pp. 594 – 600.
- Simoneau, A., Ng, E. and Elbestawi, M., 2006. "Chip formation during microscale cutting of a medium carbon steel". *International Journal of Machine Tools and Manufacture*, Vol. 46, No. 5, pp. 467 – 481.
- Simoneau, A., Ng, E. and Elbestawi, M., 2007. "Grain size and orientation effects when microcutting {AISI} 1045 steel". *{CIRP} Annals - Manufacturing Technology*, Vol. 56, No. 1, pp. 57 – 60.

22nd International Congress of Mechanical Engineering (COBEM 2013)
November 3-7, 2013, Ribeirão Preto, SP, Brazil

Tlusty, J. and MacNeil, P., 1975. "Dynamics of cutting in end milling". *Annals of CIRP*, Vol. 24, pp. 213 – 221.

Vogler, M.P., Kapoor, S.G. and DeVor, R.E., 2004. "On the modeling and analysis of machining performance in microendmilling, part ii: Cutting force prediction". *Journal of Manufacturing Science and Engineering*, Vol. 126, pp. 695 – 705.

Vollertsen, F., Biermann, D., Hansen, H., Jawahir, I. and Kuzman, K., 2009. "Size effects in manufacturing of metallic components". *{CIRP} Annals - Manufacturing Technology*, Vol. 58, No. 2, pp. 566 – 587.

8. RESPONSIBILITY NOTICE

The authors are the only responsible for the printed material included in this paper.